JOURNAL OF MATERIALS SCIENCE: MATERIALS IN MEDICINE 8 (1997) 395–401

Effects of deproteinization and ashing on site-specific properties of cortical bone

J. J. BROZ, S. J. SIMSKE*, W. D. CORLEY, A. R. GREENBERG
Departments of Mechanical Engineering and Aerospace Engineering, University of Colorado, Boulder, CO 80309-0427, USA

Buffered sodium hypochlorite (NaOCl) solution was used to remove selectively the collagen phase from bovine cortical bone. Changes in the mechanical behaviour and material properties were studied over a wide range of resolution (from 5 μm to 3 mm) using an integrated combination of experimental techniques. Optical microscopy indicated that timed immersion in NaOCl results in cortical bone specimens that consist of a mineralized tissue core surrounded by a layer of deproteinized or anorganic bone. With increased NaOCl treatment, the mechanical behaviour in three-point flexure of the intact specimens became increasingly characteristic of a brittle ceramic material. Localized material properties were evaluated using histology, scanning electron microscopy and microhardness testing. The site-specific properties and the mineralization of the cores were not significantly affected by the treatment; however, the interactions and structural framework of the hydroxyapatite crystallites within the anorganic material were compromised. This destruction of crystallite interlocking was not observed in samples in which the organic phase was removed by ashing at 800°C. The ashed samples maintained microhardness values three times those of the bleached samples. Because of its damaging effects on cortical bone structural integrity, the NaOCl treatment did not provide a reasonable means of studying, as a function of the phasic mass fraction, incremental changes in bone mechanical behaviour or the relative roles of collagen and mineral within the structural hierarchy.

1. Introduction

Cortical bone is a complex hierarchical composite material [1–3] composed of mineral, organic matrix and water phases [4, 5]. During cortical bone development, type I collagen is laid down before mineralization [6] and provides the structural framework around which hydroxyapatite (HAP) crystallites form [7]. These crystallites, in turn, largely dictate the overall bone mechanical stiffness [8]. Changes in bone mechanical behaviour have been related to the mineral phase fraction by Currey [9, 10] using samples taken from different animal species with differing histologies.

The dependence of mechanical behaviour on the phasic fractions has also been evaluated using bones obtained from a single species subjected to selective in vitro chemical treatments. Immersion in aqueous supersaturated ethylenediaminetetraacetic acid (EDTA) chelates the mineral phase while preserving the structural and mechanical properties of the collagen phase [11, 12]. Using timed immersion in an EDTA buffer solution, Sasaki and Yoshikawa [13] attempted to evaluate the properties of bovine cortical bone as a function of mineral content. Burstein *et al.* [14] and Broz *et al.* [15], however, demonstrated that such immersion results in the formation of discrete regions of demineralized and mineralized tissue rather than a uniform mineral distribution. Conversely, the collagen phase fraction can be altered with a 5.25% aqueous sodium hypochlorite (NaOCl) solution [16]. Extended immersion in NaOCl results in the removal of 99% of the collagen matrix whereby the bone ultrastructure is destroyed but the crystal structure and integrity of the mineral phase are presumably unaffected [17]. Guzelsu and Walsh [18] used this treatment to study the bioelectric signals generated by fully deproteinized (anorganic) cortical bone specimens subjected to low mechanical stresses. Overall, however, little information is available regarding the effects of NaOCl treatment on the mechanical behaviour and site-specific properties of cortical bone.

The mineral phase of cortical bone primarily consists of HAP crystallites ($[Ca_{10}(PO_4)_6](OH)_2$), together with relatively small amounts of amorphous calcium phosphates and carbonates [19]. Biologically active calcium phosphates, such as tricalcium phosphate [20], HAP [21] and coralline (coral-like) HAP [22, 23] are being increasingly utilized for bone replacement and reconstruction. The biocompatibility of these implant materials is directly affected by the composition, structure and site-specific properties of the surrounding cortical bone tissue [21].

The objective of the present study is to use timed NaOCl immersion to remove selectively the collagen

0957–4530

TABLE I Cortical bone structural hierarchy as adapted from Park [1], Katz [2], Lakes [3] and Broz *et al.* [15], where three-point flexure, microhardness, optical microscopy and scanning electron microscopy were used to evaluate the bone structures at the greater than 1 mm, 50–100 μm, 0.05–5 μm and 1–2 μm scales of resolution, respectively

Hierarchical level	Structure	Size scale
Flexure sample	Compact bone	3.6 mm × 3.6 mm × 40.0 mm
Osteons and laminae	Fibre and lamina	250 μm
Haversian canals	Pore	50–100 μm
Osteocyte lacunae	Pore	5–15 μm
Lamellae	Lamina	5 μm
Collagen fibres	Fibre	1–2 μm
HAP crystallite	Particle	0.005–0.05 μm

phase within the cortical bone structural hierarchy (Table I) and to evaluate the effects on the mechanical behaviour using macroscopic and microscopic experimental techniques [15]. In order to provide a comprehensive comparison, the site-specific properties of the NaOCl-treated tissue are also evaluated with respect to ashed cortical bone tissue and coralline HAP. Absence of the collagen framework (1–2 μm level) is hypothesized to affect directly the bone properties and possibly to provide insights for evaluating the interactions between the mineral and collagen phases.

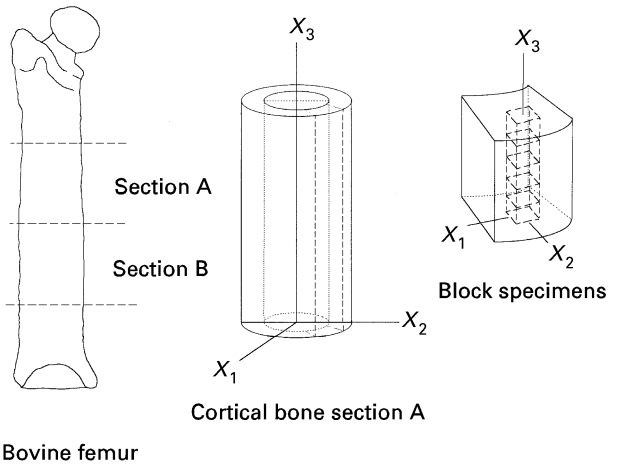

Figure 1 The orientation of the block cortical bone samples that were removed from the mid-diaphysis of a fresh bovine femur. The coordinate reference axes were maintained throughout the fabrication processes and the mechanical testing.

2. Materials and methods

Cortical bone sections were removed from the mid-diaphyseal region of several fresh bovine femora using a band saw (Fig. 1). Flexure specimens (3.6 mm × 3.6 mm × 40.0 mm) in which the long axis of the sample was parallel to the bone length were fabricated using a standard milling machine and a water- cooled low-speed saw. The specimens were frozen (− 20°C) until chemical treatment and testing.

The collagen content of the specimens was altered via deproteinization in 5.25% NaOCl, pH balanced to 7.0 using hydrochloric acid (HCl). The specimens (n = 7-10 per group) were removed after 0 (control), 1, 3, 7, 14 and 21 days. The NaOCl solution was maintained at 22 °C and replaced with fresh solution every 3–5 days. Following immersion, the specimens were rinsed in running water for approximately 1 h and frozen (− 20°C) until testing.

The specimens were thawed in distilled water and tested in three-point flexure using an Instron model 1331 servohydraulic testing system (Instron Corporation, Canton, MA) mounted with a three-point bending fixture (supports of 2 mm diameter; effective span, 37.5 mm). During testing, the maximum engineering strain rate, $d\varepsilon/dt$, at the midspan extreme fibres was approximately $1 \times 10^{-4}\,\text{min}^{-1}$. Following fracture, the cross-sectional dimensions were measured within 0.5 mm of the fracture plane. The elastic modulus, E, the stresses, σ, and the strains, ε, were obtained using classical beam theory [24]:

$$E = \frac{L^3 S}{48 I_{xx}},\ \sigma = \frac{PLz}{8 I_{xx}},\ \varepsilon = \frac{6\delta z}{L^2} \qquad (1)$$

where S (kN m^{-1}) is the stiffness, P (N) is the applied load, δ (mm) is the deflection, L (= 37.5 mm) is the effective span, I_{xx} (mm^4) is the moment of inertia and z (mm) is the specimen thickness. Custom software was used to determine the initial departure from linearity, or the proportional limit, in the load–deflection curve. The values of the elastic stress σ_e, and elastic strain, ε_e, were then determined using a greater than 0.2% strain offset criterion. Ultimate stress, σ_u and ultimate strain, ε_u, were calculated to facilitate comparisons with published bovine cortical bone data. The wet densities of the fractured specimens were obtained using Archimedes' principle [25].

Specimen composition was determined from thin sections (about 2 mm thick) apposed to the fracture surface (within 0.5 mm). The sections were weighed to determine the fully hydrated mass, M_{wet}, and dried at 70 °C for 24 h ($M_{70\,°C}$) to remove unbound water ($M_{H_2O\ unbound}$) [26]. The sections were defatted with acetone, rinsed in distilled water, redried at 70 °C for 24 h, and the mass redetermined ($M_{70\,°C\ defat}$). Finally, the sections were dried at 105 °C for 24 h to remove the bound water ($M_{H_2O\ bound}$) [26] and the mass redetermined ($M_{105\,°C}$); they were then ashed in a furnace at 800 °C for 24 h to determine the mineral mass, M_{min}. The unbound water, bound water, total water, fat, mineral and collagen masses were then expressed as percentages of M_{wet} as described in [15].

Additional sections were cut from all the specimens, air dried (22 °C and 20% relative humidity) and embedded (Buehler Epo-Thin epoxy). Several sections from the specimens NaOCl treated for 0, 14 and 21 days were ashed at 800 °C and embedded. Sections approximately 400 μm thick were cut from each embedded specimen, mounted on a glass slide with cyanoacrylate, ground to a thickness of 100 μm and dehydrated using a standard ethanol series. The specimen morphologies (at 250 × light magnification) were evaluated after staining using a standard haemotoxylin–eosin histological protocol.

The exposed surface of each embedded specimen was polished on various grades of wet–dry silicon carbide paper (180–600 grit) and wheel polished with a napped cloth impregnated with 6 μm diamond paste. Microhardness measurements were obtained using a Tukon model MO microhardness tester (Wilson Mechanical Instruments Division, Bridgeport, CT) with a 136° pyramid-shaped (Vickers) diamond indenter and a 50 gf load [27, 28]. The sections were indented along the X_1 and X_2 directions (Fig. 1) at least 12 times, each starting from the epoxy and terminating at the centre of the section. The lengths of the pyramid diagonals were measured (at 250 × magnification) and the Vickers hardness was calculated using the standard formula [27].

The sections of unashed and ashed samples NaOCl treated for 0, 14 and 21 days were repolished after microhardness testing, sputter coated with a thin layer of carbon and evaluated using a JEOL JXA-8600 Superprobe electron microprobe. The section morphologies were imaged across the epoxy tissue interface and along the X_1 and X_2 directions (Fig. 1), starting from the epoxy and terminating at the centre of the section using a 10 μm step size. An elemental analysis was performed using two separate spectrometers to determine the amounts of calcium and phosphorus in each tissue region with an analysis accuracy of ± 1%. The effects of atomic number, Z, absorbance, A, and fluorescence, F, were taken into account using the appropriate ZAF correction factors.

Several blocks of coralline HAP implant material were oven dried for 24 h at 70 and 105 °C to remove any water (unbound and bound) and the mass determined. Several blocks were ashed at 800 °C and the mineral mass determined. The mass percentages of the constituents were determined [15]. All the HAP specimens were embedded in epoxy, sectioned, polished and microhardness tested according to the aforementioned protocols.

Values for the flexural, microhardness and compositional properties were compared where appropriate using an analysis of variance (ANOVA). Differences between the groups were then evaluated using the Student's t test or Tukey's multiple comparison test as appropriate [29].

3. Results

During flexure testing of the NaOCl-treated specimens, the deproteinized (i.e., anorganic) tissue layer cracked and spalled along the outermost surfaces at the contact points of the three-point bending fixture. Beneath the spalled anorganic layer, a region of apparently unaffected cortical bone was observed at 10 × magnification. In general, all the flexural properties of the intact samples (which were normalized by the geometric properties of the entire cross-section) were affected by the presence of cracks in the anorganic tissue layer (Table II). The values for the elastic modulus, E, elastic stress, σ_e, and elastic strain, ε_e,

TABLE II Material and composition data for NaOCl-treated intact flexure specimens, where the stress and strain properties were calculated from the load–displacement curves and the composition data were obtained from sections cut from a point no greater than 2 mm from the fracture site (data are presented as mean value ± standard deviation)

	Values for the following NaOCl treatment time				
	Control	1 day	3 days	7 days	21 days
Material properties					
Number of samples	7	3	3	3	3
E (GPa)	12.8 ± 1.7^{a}	10.8 ± 1.3^{a}	10.8 ± 0.3^{a}	6.71 ± 0.17^{b}	4.71 ± 1.50^{b}
σ_e (MPa)	123.8 ± 17.3^{a}	122.2 ± 13.0^{a}	124.7 ± 8.5^{a}	51.0 ± 7.2^{b}	13.6 ± 5.9^{c}
ε_e (10^{-3} mm^{-1})	9.8 ± 1.9^{ab}	11.3 ± 0.5^{b}	11.6 ± 0.6^{b}	7.6 ± 1.1^{a}	3.3 ± 2.01^{c}
σ_u (MPa)	205.4 ± 40.7^{ab}	162.0 ± 17.1^{b}	168.2 ± 1.4^{b}	72.6 ± 8.3^{b}	27.0 ± 4.6^{c}
ε_u (10^{-3} mm^{-1})	20.4 ± 4.8^{a}	18.9 ± 1.4^{a}	18.6 ± 1.4^{a}	17.1 ± 1.5^{a}	7.4 ± 0.3^{c}
Composition					
Number of samples	7	3	3	3	3
Unbound H_2O mass %	11.7 ± 0.8^{a}	14.0 ± 0.6^{a}	13.2 ± 0.1^{a}	15.0 ± 6.0^{b}	23.2 ± 6.9^{c}
Bound H_2O mass %	1.3 ± 0.4^{a}	1.0 ± 0.3^{a}	0.8 ± 0.2^{a}	1.0 ± 0.4^{a}	0.6 ± 0.2^{a}
Fat mass %	0.2 ± 0.2^{a}	0.1 ± 0.1^{a}	0.4 ± 0.2^{a}	0.8 ± 0.1^{a}	0.5 ± 0.4^{a}
Total H_2O mass %	13.0 ± 0.7^{a}	15.0 ± 0.4^{b}	14.0 ± 0.2^{b}	16.0 ± 5.9^{a}b	23.8 ± 6.8^{c}
Mineral mass %	61.5 ± 0.7^{a}	62.0 ± 0.5^{a}	61.5 ± 0.3^{a}	65.7 ± 5.8^{b}	64.3 ± 5.8^{b}
Collagen mass %	25.3 ± 0.4^{a}	22.9 ± 0.2^{b}	24.1 ± 0.2^{a}	17.5 ± 0.2^{c}	11.4 ± 0.5^{d}
Ash mass %	70.9 ± 0.3^{a}	73.1 ± 0.3^{b}	71.8 ± 0.2^{a}	78.9 ± 1.3^{c}	85.0 ± 0.5^{d}
Calcium mass%	28.2 ± 0.1^{a}	29.1 ± 0.1^{b}	28.6 ± 0.1^{a}	31.4 ± 0.5^{c}	33.8 ± 0.2^{d}

Statistics: where appropriate in all the tables, superscript bold letters (and in the figures bold letters) are used to indicate groups that are significantly different. If two groups share any bold letter in common, then they are not significantly different ($p < 0.05$) using Tukey's multiple range test for pair wise comparisons. If two groups do not have any bold letter in common, then they are significantly different ($p < 0.05$).

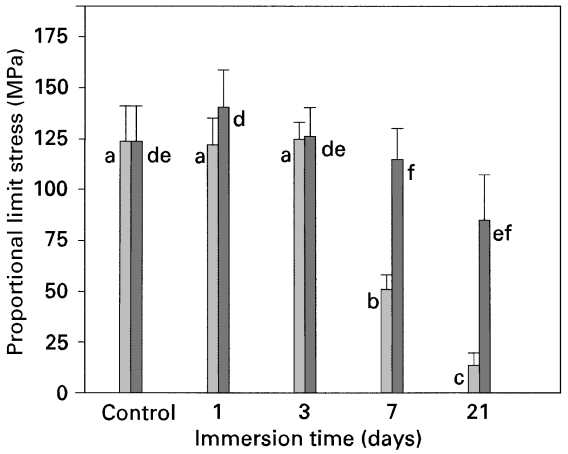

Figure 2 Changes in the elastic stress, σ_e, plotted with respect to NaOCl immersion times for the intact (□) and core (■) specimens. Statistical comparisons are made within the intact and core specimen groups and not between the two groups. Although not initially statistically significant for the core specimens, σ_e tended to decrease with increasing immersion time; however, the changes were more pronounced in the intact specimens. The control values for the intact and core specimens are identical. The data are plotted as mean value $\pm$ standard deviation.

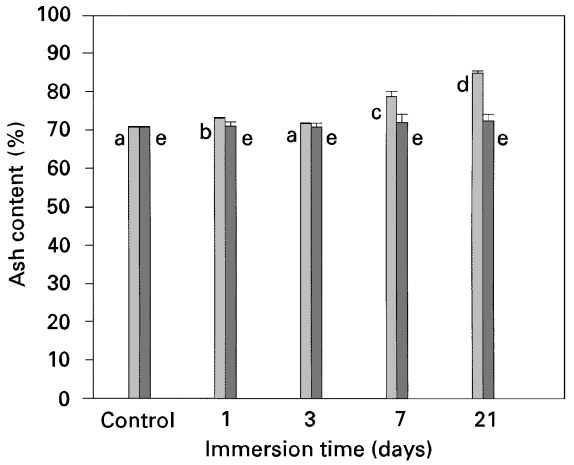

Figure 3 Changes in the mineralization plotted with respect to the NaOCl immersion times for the intact (□) and core (■) specimens. Statistical comparisons are made within the intact and core specimen groups and not between the two groups. With longer immersion times, the ash content of the intact specimens systematically increased while the core composition remained unaffected. The control values for the intact and core specimens are identical. The data are plotted as mean value $\pm$ standard deviation.

significantly decreased with extended immersion in the NaOCl solution (Fig. 2). The trends observed for the ultimate stress, σ_u, and ultimate strain, ε_u, were similar to those observed for the elastic properties.

The percentage of collagen in the NaOCl-treated samples decreased significantly at each immersion time interval (Table II). After 21 days, the average collagen content and mineral content had decreased by 55% and increased by 16%, respectively, from the control values (Fig. 3). The unbound-H_2O content increased from 11.7% (control) to 23.2% for the 21 day NaOCl-treated intact samples. Concomitantly, the total-H_2O content of the 21 day NaOCl-treated intact samples increased by 177% compared to the

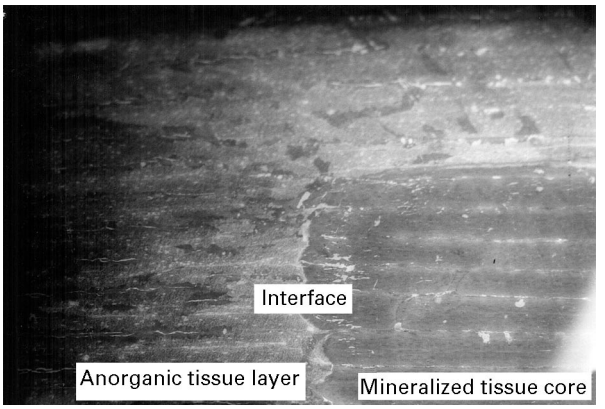

Figure 4 Micrograph (at 250 × magnification) of a representative cross-section taken from a 21 day NaOCl-treated flexure sample. The mineralized core, the discrete interface and the anorganic tissue layer can be clearly distinguished. Extensive microcracking which resulted from the chemical treatment is visible between the lamellae of the anorganic tissue. Such structural damage was not observed within the tissue of the mineralized core.

control sample. However, an overall decreasing trend was observed for the bound-H_2O content. The fat content was relatively unaffected by the chemical treatment.

Optical microscopy (at 125 × magnification) and histological analysis (at 250 × magnification) of NaOCl-treated cross-sections showed a mineralized core surrounded by a discrete layer of anorganic bone tissue (Fig. 4). Within each tissue region, osteocyte lacunae were clearly visible and the vascular channels (i.e., Haversian and Volksmann canals) appeared to be continuous across the interface; however, the anorganic tissue region was extensively cracked and structurally heterogeneous (Fig. 4). In the haemotoxylin –eosin stained sections, a significant cellular gradient between the tissue regions was not observed. The size of the anorganic tissue region increased with extended immersion and the percentage of mineralized tissue area decreased to 26.9 $\pm$ 1.9% of the control values for the 21 day NaOCl-treated group.

The discrete interface between the mineralized and anorganic tissue regions was observed in scanning electron micrographs of representative specimens NaOCl treated for 0, 14 and 21 days. Elemental line scans of the NaOCl-treated specimens indicated that the amounts of calcium (Ca) and phosphorus (P) in both the mineralized core and the anorganic layer were comparable with those of the control. Detailed morphological comparisons of the tissue regions indicated that the structural integrity of the anorganic layer had been compromised by the chemical treatment (e.g., a large number of cracks and discontinuities were observed in the bone lamella of the anorganic tissue region). The discrete interface was also visible in scanning electron micrographs of the ashed 14 and 21 day NaOCl-treated samples, i.e., the core could be readily differentiated from the layer of anorganic bone tissue. Furthermore, the ashed mineralized core appeared to be more structurally intact than the ashed anorganic region.

A discrete interface between the mineralized core and the anorganic bone layer was visible during

TABLE III Microhardness measurements obtained from control and NaOCl-treated cortical bone sections, where the wet density of the mineralized tissue core was determined from one half of each fractured core flexure specimen (data are presented as mean value ± standard deviation; NA means not applicable, i.e., an anorganic bone layer was not present in the control samples)

	Values for the following NaOCl treatment names					
	Control	1 day	3 days	7 days	14 days	21 days
Mineralized core						
Wet density (g cm^{-3})	2.03 ± 0.03[a]	2.01 ± 0.02[a]	2.01 ± 0.03[a]	2.00 ± 0.05[a]	2.03 ± 0.04[a]	1.92 ± 0.04[b]
Number of indents	21	NA	15	13	11	11
(Vickers hardness (kgf mm^{-2})	69 ± 5	NA	66 ± 6	71 ± 6	73 ± 6	72 ± 8
Anorganic bone tissue						
Number of indents	NA	—	19	19	12	14
(Vickers hardness (kgf mm^{-2})	NA	—	33 ± 12	36 ± 19	33 ± 12	42 ± 14

TABLE IV Material and composition data for NaOCl-treated core flexure specimens, where the stress and strain properties were calculated from the load–displacement curves and the composition data were obtained from sections cut from a point greater than 2 mm from the fracture site (data are presented as mean value ± standard deviation)

	Values for the following NaOCl treatment times					
	Control	1 day	3 days	7 days	14 days	21 days
Material Properties						
Number of samples	7	7	6	7	5	7
E (GPa)	12.8 ± 1.7[ab]	13.5 ± 1.2[ab]	13.4 ± 1.0[ab]	14.2 ± 1.3[ab]	16.1 ± 1.1[a]	11.5 ± 2.2[b]
σ_e (MPa)	123.8 ± 17.3[ab]	140.7 ± 18.1[a]	126.3 ± 13.9[ab]	114.8 ± 15.4[ab]	110.4 ± 7.0[b]	85.0 ± 22.3[c]
ε_e (10^{-3} mm^{-1})	9.8 ± 1.9[a]	10.5 ± 1.6[ab]	9.5 ± 1.4[ab]	8.1 ± 1.1[ab]	6.8 ± 0.9[c]	7.4 ± 1.1[bc]
σ_u (MPa)	205.4 ± 40.7[a]	151.6 ± 67.4[ab]	178.9 ± 15.8[ab]	156.1 ± 11.6[ab]	152.9 ± 5.0[ab]	121.0 ± 22.0[b]
ε_u (10^{-3} mm)	20.4 ± 4.8[a]	16.3 ± 2.0[ab]	17.2 ± 0.9[ab]	15.1 ± 2.2[ab]	12.1 ± 0.5[b]	14.8 ± 1.3[ab]
Core Composition						
Number of samples	7	7	7	7	7	7
Unbound H_2O mass %	11.7 ± 0.8[a]	12.9 ± 0.7[a]	11.7 ± 0.5[a]	11.4 ± 0.9[a]	11.7 ± 0.7[a]	15.5 ± 4.0[b]
Bound H_2O mass %	1.3 ± 0.4[a]	1.0 ± 0.5[a]	0.9 ± 0.4[a]	1.0 ± 0.4[b]	1.6 ± 0.6[c]	2.3 ± 0.5[b]
Fat mass %	0.2 ± 0.2[a]	0.3 ± 0.2[a]	0.7 ± 0.3[a]	0.6 ± 0.2[a]	0.7 ± 0.4[a]	0.4 ± 0.3[a]
Total H_2O mass %	13.0 ± 0.7[a]	13.9 ± 0.8[a]	12.6 ± 0.6[a]	12.4 ± 1.1[a]	13.3 ± 1.0[a]	17.9 ± 3.7[b]
Mineral mass %	61.5 ± 0.7[a]	61.1 ± 0.9[a]	61.6 ± 0.7[a]	62.7 ± 1.8[a]	61.8 ± 1.5[a]	59.3 ± 2.9[b]
Collagen mass %	25.3 ± 0.4[a]	24.8 ± 1.0[a]	25.1 ± 0.7[a]	24.2 ± 0.7[a]	24.2 ± 1.0[a]	22.4 ± 1.8[b]
Ash mass %	70.9 ± 0.3[a]	71.2 ± 1.0[a]	71.0 ± 0.9[a]	72.1 ± 1.1[a]	71.9 ± 1.3[a]	72.6 ± 1.7[a]
Calcium mass %	28.2 ± 0.1[a]	28.3 ± 0.4[a]	28.3 ± 0.3[a]	28.7 ± 0.4[a]	28.6 ± 0.5[a]	28.9 ± 0.7[a]

microhardness evaluation. The microhardness values of the control and NaOCl-treated sample cores ranged from 66 to 73 kgf mm^{-2} (Table III) and the microhardness of each NaOCl-treated sample mineralized core was not statistically different from that of the control. In the anorganic bone layer, the values for microhardness (ranging from 33 to 42 kgf mm^{-2}) were approximately 50% lower and significantly different ($p < 0.05$) from the control value. The microhardness of the ashed control sample was based on 15 measurements across the cross-section and found to be 115 ± 7 kgf mm^{-2}. In contrast, the microhardness values of the pre-ashed and post-ashed coralline HAP samples were significantly different (i.e., 253 ± 12 kgf mm^{-2} and 286 ± 24 kgf mm^{-2}, respectively).

To investigate further the effects of NaOCl immersion on the core properties, the anorganic portions of the rectangular specimens were carefully removed with a scalpel ($n = 5$–7 for the flexure sample, NaOCl treated 1, 3, 7, 14 and 21 days). The remaining mineralized tissue cores were mechanically tested and compositionally evaluated. Following mechanical testing, the cross-sectional properties of the core specimens were determined and the stress–strain properties were calculated (Table IV).

Overall, the elastic moduli for all the core specimen groups were not significantly affected by the NaOCl immersion. The values of elastic stress, σ_e, for the 1, 3 and 7 day groups were not statistically different from those of the control group. Although not initially significant, an overall decreasing trend for the elastic stress was observed for the extended immersion times (Fig. 2). Values of σ_e and σ_u for 21 day NaOCl-treated specimens were 31% and 41% lower, respectively, than the control. The elastic strains, ε_e, of the 14 and 21 day NaOCl-treated groups were significantly lower than those of the control group. Similarly, the ultimate strain demonstrated a decreasing trend with extended immersion time.

The mineral content and collagen content of the core specimens were not significantly affected by the chemical treatment until the 21 day NaOCl-treated group. For the 21 day group, the mineral content and collagen content were 5% and 12% lower, respectively, than the control values. However, for the ash content, no statistically significant differences were

observed (Fig. 3). The unbound-H_2O content and total-H_2O content of the 21 day NaOCl-treated core group were significantly higher than all other groups and no clear trend was observed for the bound H_2O. The NaOCl treatment did not significantly affect the fat content of the cores. A decreasing trend for the wet density of the core samples was observed (Table IV); however, the differences with respect to the control groups did not become statistically significant ($p < 0.05$) until after NaOCl treatment for 21 days.

4. Discussion

Currey [10, 11] demonstrated that small changes in the ash content (mineral content normalized with respect to bone dry mass) at the smallest bone hierarchical scale, i.e., 0.005–0.05 μm, significantly affect cortical bone mechanical behaviour and material properties. Otter *et al.* [17] and Guzelsu and Walsh [18] showed that NaOCl immersion results in the removal of bone ultrastructure at the 1–2 μm level (Table I) without significantly affecting the mineral phase material and bioelectrical properties. In the current study, NaOCl deproteinization was utilized to alter the relative collagen content of bovine cortical bone specimens. The deproteinization occurred primarily along the bone–fluid interface, and to a much lesser extent within the specimen cross-section. Consequently, the flexure specimens were structurally heterogeneous and consisted of a mineralized core surrounded by an anorganic tissue layer whose thickness was governed by immersion time. As the thickness of the anorganic tissue layer increased, the flexural behaviour of the chemically treated specimens became increasingly characteristic of a ceramic material, i.e., brittle fracture at relatively low strains with little plastic deformation.

For all flexure specimens, the shear component was less than a fifteenth of the total deflection [30] and the bending stress values were corrected by a factor of 0.97 [31]. The corrected flexural properties (elastic modulus, ultimate stress and ultimate strain) and ash content (e.g., $M_{min}/M_{105\,^\circ C}$) obtained from the control group (immersion for 0 days, i.e., no immersion) were not statistically different ($p > 0.10$) from those obtained by Martin and Boardman [32] for bovine cortical bone specimens. Within the mid-diaphyseal region of bovine bone, the distal–proximal variations in elastic modulus and flexure strength are minimal [33]. Thus, the significant changes in the mechanical behaviour of the NaOCl-treated intact and core specimens with respect to the control were attributable to the chemical treatment rather than to the location or orientation within the bone. However, owing to the spalling of the anorganic tissue layer at the load point and supports, flexure testing was found to be inadequate for accurately evaluating material property changes of the NaOCl-treated intact specimens. Material property changes between these specimens were more appropriately quantified using the site-specific testing techniques.

The overall increase in the mineral content (the mineral mass normalized with respect to the specimen wet mass) of the intact NaOCl-treated specimens reflects the increase in the unbound-H_2O content in the samples and replacement of the collagen ($\rho_{wet} \approx 1.18\ g\,cm^{-3}$) with water ($\rho \approx 1.00\ g\,cm^{-3}$). Thus, as the collagen phase is removed, the resulting voids in the anorganic bone are filled with water and the total-H_2O content significantly increases. The decrease in the bound-H_2O content is presumably due to preferential adsorption of water to the collagen molecules [34]. The systematic increase in the ash content is more indicative of the mass changes in the mineral and collagen resulting from the chemical treatment. Although the collagen content and the ash content of the NaOCl-treated core specimens were relatively unaffected by extended immersion in the NaOCl, the treatment significantly affected the elastic stress and strain values and elastic flexural properties (Table IV).

Microhardness testing and scanning electron microscopy were effective in quantifying the physical effects of the chemical treatment and the small-scale structural variations across the anorganic bone layer of NaOCl-treated intact samples at the 50–100 μm level in the structural hierarchy (Table 1). Within the anorganic bone regions, the average values of the Vickers hardness were considerably lower than those of the mineralized core and control samples. Although the values of Vickers hardness of the anorganic bone were comparable among the NaOCl-treated groups, a fairly large variance (25–40% of the mean value) within each deproteinized region was observed. The average Vickers hardness of the ashed samples was considerably higher and the variance in the measurements across the cross-section was smaller (approximately 10% of the mean value) in comparison with the anorganic bone values. This difference is probably attributable to the increasingly heterogeneous appearance of the NaOCl-treated anorganic tissue regions (Fig. 4).

Ashing at high temperatures (800 °C), in contrast, removes the organic constituents (collagen and other proteins) of cortical bone and the coralline HAP without, apparently, affecting the interlocking framework of the HAP crystallites [35, 36]. Furthermore, similar to the results of Wang and Chaki [36], the ashing process increased the microhardness of both the coralline HAP and the ashed-control cortical bone. On the other hand, chemical treatment in NaOCl, as a result of either the reaction kinetics or fluid flow due to agitation, apparently weakens the HAP crystallite interactions and leads to microcracking within cortical bone. Thus, the drop in microhardness in the anorganic bone regions was not wholly the result of the collagen removal but was also apparently due to the heterogeneous destruction of the HAP crystallite support framework.

In the context of bone replacement and reconstruction, there exists the possibility of using the ashed and anorganic cortical bone tissue as implantable materials. Porous coralline HAP is a commonly used biocompatible implant material which binds with the surrounding bone tissue and allows for substantial ingrowth, given a minimum pore size of 50 μm [37]. Klawitter and Hulbert [38] found that pore sizes of

approximately 150 μm are required for optimum ingrowth. Within the ashed and anorganic cortical bone tissues, the average size of the pores ranged from approximately 50 to 200 μm. As such, the biocompatibility of bone HAP makes it a candidate for use as an implant material; however, the microhardness values of the ashed and anorganic bone HAP were considerably lower than those of the coralline HAP. Therefore, as the structural properties of the bone–implant combination are dominated by the properties of brittle implant material [22, 37], the ashed and anorganic cortical bone HAP implants may not be as suitable for bone repair as other biologically active calcium phosphates.

The NaOCl treatment was effective in removing the collagen fibres at the 1-2 μm level of the cortical bone structural hierarchy (Table I). Somewhat similar to immersion in EDTA [14, 15], the NaOCl treatment produced discrete regions of mineralized and chemically altered tissues. However, the mechanical behaviour and material properties of the mineralized cores of the NaOCl-treated samples were significantly altered. Thus, unlike EDTA treatment [15] and contrary to the hypothesis of Guzelsu and Walsh [18], immersion in NaOCl apparently does not leave the overall structural and material properties of the mineralized and anorganic tissues completely intact.

While contributing little to the hardness of bone, collagen acts as the underlying structure around which a HAP framework is constructed [39, 40]. Removal of this support structure at the 1–2 μm level, by either ashing or chemical treatment, results in a material which is highly brittle, porous and susceptible to microcracking at each level of the structural hierarchy (Figs 4 and 5). The data presented here, in fact, indicate that ashed bone demonstrates less induced damage than bleached bone, despite its known brittleness and extensive microcracking. Thus, owing to the brittle and discontinuous nature of the deproteinized bone and the effects of the treatment on the mineralized tissue, the NaOCl treatment does not provide a reasonable means of studying incremental changes in the gross mechanical behaviour of cortical bone as a function of the mineral mass fraction.

Acknowledgments

The authors acknowledge Dr John W. Drexler of the University of Colorado Department of Geological Sciences for his expert assistance in the wavelength dispersive analysis. Also, the authors recognize the contribution of Mr David M. Otten (preliminary microhardness testing) and Mr Ted Bateman (photography). The authors gratefully acknowledge the support of this research through National Aeronautics and Space Administration grant NAGW-1197.

References

1. J. B. PARK, "Biomaterials: an introduction" (Plenum, New York, 1979) p. 10.
2. J. L. KATZ, "The structure and biomechanics of bone", Proceedings of a Symposium of the Society for Experimental Biology (Cambridge University Press, Cambridge, 1980) p. 137.
3. R. LAKES, *Nature* **361** (1993) 511.
4. J. L. KATZ, *J. Biomech.* **4** (1971) 455.
5. K. PIEKARSKI, *Int. J. Engng. Sci.* **11** (1973) 557.
6. E. D. GARDNER, R. O'RAHILLY and F. MULLER, "Anatomy" (W.B. Saunders Co., Philadelphia, PA, 1986) p. 1.
7. L. WEISS, "Histology: cell and tissue biology" (Elsevier Biomedical, New York, 1983) p. 43.
8. C. W. McCUTCHEN, *J. Theor. Biol.* **51** (1975) 51.
9. J. D. CURREY, *J. Biomech.* **2** (1969) 1.
10. J. D. CURREY, *J. Biomech.* **8** (1975) 81.
11. I. R. DICKSON and S. S. JANDE, *Calcif. Tissue Int.* **32** (1980) 175.
12. C. C. DANIELSEN, T. T. ANDREASSEN and L. MOSEKILDE, L., *Calcif. Tissue Int* **39** (1986) 69.
13. N. SASAKI and M. YOSHIKAWA, *J. Biomech.* **26** (1993) 77.
14. A. H. BURSTEIN, J. M. ZIKA, K. G. HEIPLE and L. KLEIN, *J. Bone Jt Surg.* **A57 (**1975) 956.
15. J. J. BROZ, S. J. SIMSKE and A. R. GREENBERG, *J. Biomech.* **28** (1995) 1357.
16. A. BOYDE and M. HOBDELL, *Anatomy* **99** (1969) 98.
17. M. OTTER, S. GOHEEN and S. W. WILLIAMS, *J. Orthop. Res.* **6** (1988) 346.
18. N. GUZELSU and W. R. WALSH *J. Biomech.* **23** (1990) 673.
19. A. C. GUYTEN, "Textbook of medical physiology" (W.B. Saunders, Philadelphia, PA, 1981) p. 973.
20. A. UCHIDA, S. M. L. NADE, E. R. McCARTNEY and W. CHING, *J. Bone Jt Surg.* **66-B** (1984) 269.
21. R. E. HOLMES, R. W. WARDROP and L. M. WOLFORD, *J. Oral Maxillofac. Surg.* **46** (1988) 661.
22. R. CHIROFF, E. WHITE, J. WEBER and D. ROY, *J. Biomed. Mater. Res.* **6** (1975) 29.
23. R. E. HOLMES, *Plast. Reconstr. Surg.* **63** (1979) 626.
24. ANONYMOUS, "1983 Annual book of ASTM standards" (American Society for Testing and Materials, Philadelphia, PA, 1983) Standard D790M-82.
25. R. B. ASHMAN, S. C. COWIN, W. C. VAN BUSKIRK and J. C. RICE, *J. Biomech.* **17** (1984) 349.
26. R. A. ROBINSON, *Clin. Orthop.* **17** (1960) 69.
27. R. AMPRINO, *Acta Anat* **34** (1958) 161.
28. M. RAMRAKHIAMI, D. PAL and T. S. MURTY, *Acta anat.* **103** (1979) 358.
29. J. NETER and W. WASSERMAN, "Applied linear statistical models" (Richard D. Irwin, Inc., Homewood, IL, 1979) p. 313.
30. M. W. JAMESON, J. A. A. HOOD and B. G. TIDMARSH, *J. Biomech.* **26** (1993) 1055.
31. M. FROCHT, "Photoelasticity", Vol. II" (Wiley, New York, 1948) p. 112.
32. R.B. MARTIN and D. L. BOARDMAN, *J. Biomech.* **26** (1993) 1047.
33. M. H. POPE and J. O. OUTWATER, *J. Biomech.* **7** (1974) 61.
34. G. W. HASTINGS and F. A. MAHMUD, *J. Mater. Sci.: Mater. Med.* **2** (1991) 118.
35. S. C. COWIN, "Bone mechanics" (CRC Press, Boca Raton, FL, 1980) p. 97.
36. P. E. WANG and T. K. CHAKI, *J. Mater. Sci.: Mater. Med.* **4** (1993) 150.
37. R. M. PILLIAR, *J. Biomed. Mater. Res.* **21(A1)** (1987) 1.
38. J. J. KLAWITTER and S. F. HULBERT, *J. Biomed. Mater. Res. Symp.* **2** (1971) 161.
39. S. LEES, *Calcif. Tiss. Int.* **27** (1979) 53.
40. S. LEES, *J. Biomech.* **14** (1980) 561.

Received 31 May 1995
and accepted 18 September 1996